



In situ synthesis of cross-linking gel polymer electrolyte for lithium metal batteries

Jiaxin Chen¹ · Longxuan Wang¹ · Zhipeng Huang¹ · Yuxuan Liang¹ · Juntian Qu² · Ziqiang Wang¹ 

Received: 24 April 2024 / Revised: 6 June 2024 / Accepted: 12 June 2024 / Published online: 19 June 2024
© The Author(s) 2024

Abstract

The room temperature ionic conductivity of polyethylene oxide (PEO)-based polymer electrolytes is low, the electrochemical window is narrow, and the mechanical strength is relatively poor. In this work, a cross-linking gel-based solid composite polymer electrolyte (CG-SCPE) was synthesized by introducing electrochemically stable carbonate-based functional groups. The synthesized CG-SCPE presents excellent tensile strength (26 MPa) and a wide electrochemical stability window (> 4.5 V vs. Li/Li⁺). Meanwhile, the in situ polymerization method induced by thermal heating resulted in good compatibility between electrodes/electrolytes. In addition, the assembled LiNi_{0.5}Co_{0.2}Mn_{0.3}O₂/CG-SCPE/Li battery exhibited satisfactory electrochemical performance. Therefore, the gel polymer electrolyte CG-SCPE with cross-linking network provides the possibility for future application of safe and high-performance solid-state lithium metal batteries. The results indicate that the introduction of cross-linking framework can simultaneously improve the mechanical strength, thermal stability, and electrochemical performance of solid polymer electrolyte.

Keywords In-situ polymerization · Cross-linking gel polymer electrolyte · Lithium metal batteries

Introduction

Owing to the increasing demand for energy storage of safety, high energy density, and long cycling life, solid state lithium metal battery has experienced unprecedented development, aiming to replace the currently used lithium ion batteries [1, 2]. Solid electrolytes could potentially inhibit the lithium dendrite penetration and possess the merit of safety, compared with the volatile and flammable liquid electrolytes [3]. In particular, compared with inorganic solid electrolytes, solid polymer electrolytes (SPE) have several advantages, including simple synthesis process, feasibility of mass production, excellent interfacial compatibility between electrodes and electrolytes, and high mechanical strength [4].

Therefore, SPE emerges as the promising electrolyte for further practical employment of solid-state lithium batteries [5, 6]. The abundant and inexpensive raw materials used to fabricate SPE also enables the ample supply for the large-scale industrialization of solid-state lithium batteries [7, 8].

Commonly employed preparation methods for SPE include casting method [9, 10], phase inversion method [11, 12], and electro-spinning method [13, 14]. However, these ex situ methods possibly lead to significant interfacial gaps between electrodes and electrolytes in batteries [15, 16]. It will generate large interfacial impedance and severely affect the electrochemical performance. The in situ polymerization, however, could alleviate the interfacial contact problem, as well as eliminate the complex processes of ex situ polymerization [17]. The precursor materials chosen for in situ polymerization have certain requirements, including mild initiation conditions and selected reaction process with little gas production [18–20]. During in situ polymerization process, monomers or oligomers would undergo transformation into large molecular triggered by light exposure or thermal heating [21–24]. By employing the in situ polymerization technique, SPE with excellent interface performance, high energy density, and enhanced safety can be obtained [25].

Jiaxin Chen and Longxuan Wang contributed equally to this work.

✉ Ziqiang Wang
wangziqiang@sz.tsinghua.edu.cn

¹ Institute of Materials Research, Shenzhen International Graduate School, Tsinghua University, Shenzhen 518000, Guangdong, China

² Shenzhen International Graduate School, Tsinghua University, Shenzhen, China

Since its inception in the 1970s, polyethylene oxide (PEO)-based electrolytes have emerged as the most extensively researched materials within the realm of polymer electrolytes [26]. Its ionic conductive mechanism involves a continuous series of complexation and dissociation reactions between lithium ions and oxygen atoms existed in the ethylene oxide unit structure. Presently, the primary obstacles facing PEO-based polymer electrolytes encompass diminished room temperature ionic conductivity, inadequate mechanical characteristics, narrow electrochemical window, and high interfacial impedance. The quest for enhancing the performance of PEO-based polymer electrolytes has been ongoing for years. For example, the addition of polycationic ionic liquids to the PEO matrix allows for an increased proportion of amorphous PEO and promotes the dissociation of lithium salts, thereby resulting in an improvement in ionic conductivity; blending PEO with polymers with better mechanical properties can improve the mechanical properties of solid polymer electrolytes and reduce crystallinity; by molecular design, PEO is subjected to grafting copolymerization, block copolymerization, and other methods to adjust its molecular structure, enabling the polymer electrolyte to simultaneously enhance its ionic conductivity and mechanical properties [4, 27]. Furthermore, the application of $\text{Li}_{1.4}\text{Al}_{0.4}\text{Ti}_{1.6}(\text{PO}_4)_3$ (LATP) coating on the surface of the LiCoO_2 cathode can effectively alleviate surface catalysis, extending the stable operating voltage to > 4.5 V [28]. The high-modulus polyimide (PI) membrane can act as a mechanical support in composite solid electrolytes, preventing dendrite penetration and avoiding battery short circuits [29]. However, the ionic conductivity of PEO-based electrolytes at room temperature is still inferior to liquid electrolytes and inorganic solid electrolytes [8]. Also, the interfacial compatibility between anode and solid electrolyte hinders the development of solid-state batteries [30]. In order to achieve acceptable interfacial compatibility and high room temperature ionic conductivity of polymer electrolytes without compromising their mechanical performance and safety, numerous studies have been conducted to develop a simple and effective strategy. Cross-linked polymer electrolytes are viable solution to address these issues. Functional methacrylates are commonly introduced into PEO to provide reaction sites for radical initiated polymerization [31, 32]; it is precisely due to the presence of ester functional groups that polymer electrolytes are endowed with higher electrochemical performance [33]. Compared with traditional PEO-based solid state electrolytes, polycarbonate-based electrolytes are a focus of attention in the field of solid-state polymer electrolytes due to their excellent electrochemical performance and better compatibility with anodes [34–37].

Based on previous studies, this work aims to utilize a cross-linking structure as the skeleton for the polymer electrolyte to enhance its mechanical strength. Combining with

in situ polymerization technology is proposed to address interfacial compatibility issues at the solid-solid interface. The polymer obtained by introducing polyethylene glycol diacrylate (PEGDA) as a crosslinking monomer into PEO exhibits improved mechanical properties. Meanwhile, the presence of PEO makes the electrolyte highly flexible. In the process of solid state battery assembly, PEGDA in the precursor solution is in situ polymerized under free radical initiation to form CG-SCPE crosslinked gel polymer electrolyte. The in situ polymerized CG-SCPE forms compatible contacts at the interfaces for the cathode and anode, significantly reducing interfacial impedance and thus enhancing the electrochemical performance of solid-state lithium batteries [34].

Materials and characterization

Chemicals

All chemical reagents used in the experiment, polyethylene oxide (PEO), polyethylene glycol (PEG), polyethylene glycol diacrylate (PEGDA), and AIBN, were purchased from Macklin Inc.

CG-SCPE gel electrolyte synthesis

Cross-linking of C-SCPE polymer membrane

For initial solution preparation, first, dissolve PEO into acetonitrile with 8 wt% ratio, and add LiTFSI salt with mass ratio of EO: Li reaching 12:1 (EO is ether oxygen unit). Second, further add PEGDA to PEO solution with a mass ratio of 3:2 between PEO and PEGDA, and add 0.1% AIBN as the initiator, followed by magnetic stirring.

For membrane fabrication, apply the evenly stirred solution into the PI film as membrane skeleton, and dry it at 70 °C for 12 h to obtain the cross-linked SCPE (C-SCPE) electrolyte membrane.

In situ polymerization to prepare CG-SCPE gel electrolyte

For in situ polymerization, we need to prepare the precursor solution, for which 30 wt% PEG is first introduced into the cross-linking PEGDA monomer of 20 wt% and 50 wt% electrolyte is further added with 0.1 wt% AIBN as the initiator. The electrolyte parameters are 1.0M LiPF_6 in EC:DMC = 1:1 Vol% with 5% FEC.

During solid-state battery assembling, the precursor solution is dip coated onto C-SCPE membrane with further in situ heating polymerization at 60 °C for 12 h. The cross-linking gel polymer electrolyte of CG-SCPE is prepared well after the in situ polymerization. Such in situ polymerization

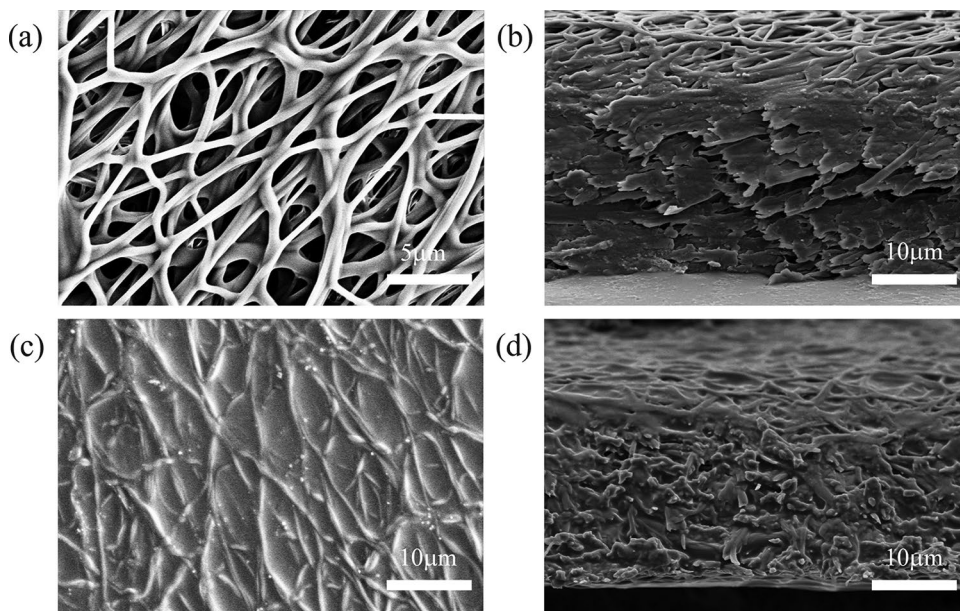
Results and discussion

For in situ polymerization, 2,2-Azobis(2-methylpropionitrile) (AIBN) can be employed to initiate macromonomer, which is an efficient thermal initiator for free radical polymerization. The FTIR spectrum in the Fig. S1 shows that after thermal-heating induced in situ polymerization, the absorption peak corresponding to the C=C double bond located at 1634 cm^{-1} disappears. This indicates that the C=C double bond transforms into a C-C single bond at the end of the cross-linked monomer. Free radicals could initiate polymerization to form a large number of cross-linked networks, which can improve the mechanical strength of polymer electrolytes. Specifically, the stress-strain curve shown in Fig. S2 indicates that CG-SCPE film presents an excellent mechanical strength of 26 MPa under compression with 36% strain, which is much larger than that of PEO film of ~ 5 MPa. Before in situ polymerization, C-SCPE membrane is tested to compressed to a similar strain of 35% under a larger compressive stress of 34 MPa. It indicates that CG-SCPE, as a cross-linked gel polymer electrolyte manifests better flexibility compared with C-SCPE. Besides, the cross-linking gel polymer electrolyte has a thickness of about $30\text{ }\mu\text{m}$, as seen in cross-section image of Fig. 2d.

Thermogravimetric analysis (TGA, Fig. S3) is performed and shows that the 5% mass loss of CG-SCPE reaches at temperature of $115\text{ }^\circ\text{C}$. When the temperature rises to around $250\text{ }^\circ\text{C}$, the mass drops sharply to 85%, mainly due to the volatilization of the small molecule plasticizer EC ($T_b = 248\text{ }^\circ\text{C}$). For C-SCPE, due to the absence of plasticizers, the temperatures for mass losses of 5% and 85% are higher than those of CG-SCPE.

The ionic conductivity of the electrolyte increases with the added amount of liquid electrolyte in the polymer electrolyte system, as shown in Fig. 3. To achieve CG-SCPE with an ionic conductivity greater than 10^{-4} S cm^{-1} at $25\text{ }^\circ\text{C}$, the liquid electrolyte (1.0M LiPF₆ in EC:DMC = 1:1 Vol% with 5%FEC) was chosen with a mass ratio of 50% relative to CG-SCPE. Figure 3a shows the relationship between the ion conductivity of CG-SCPE and temperature change. At room temperature of $25\text{ }^\circ\text{C}$, it could reach a high ionic conductivity of $1.38 \times 10^{-4}\text{ S cm}^{-1}$. The glass transition temperature (T_g) of PEO is very low of about $-64\text{ }^\circ\text{C}$, and the introduction of electrolyte as a plasticizer will further reduce the glass transition temperature. Thus, the ionic conductivity of polymer electrolyte follows the Vogel-Tamman-Fulcher (VTF) rule, rather than Arrhenius type behavior. The electrochemical stability of the electrolyte was evaluated by linear sweep voltammetry (LSV) and cyclic voltammetry (CV), as shown in Fig. 3b, c. In Fig. 3b, for PEO-based polymer electrolytes, the oxidation current in LSV begins to rise at around 4.5 V (relative to Li/Li⁺), corresponding to the oxidative decomposition of PEO. In contrast, cross-linked polymer electrolytes still remain electrochemical stability at 4.8 V, indicating that introducing electrochemically stable ester functional groups into the polymer skeleton can improve the oxidation stability of the polymer electrolytes. The cyclic voltammetry curve, as shown in Fig. 3c, shows that lithium metal exhibits stripping occurred at around 0.6 V (vs. Li⁺/Li) and begins to deposit at -0.3 V (vs. Li⁺/Li). Due to the absence of other oxidation peaks below 4.5 V (vs. Li⁺/Li), and the reversible deposition and stripping process, the cross-linked polymer electrolyte CG-SCPE

Fig. 2 Morphology characterization of CG-SCPE. **a** Surface morphology of PI film; **b** morphology for cross section of PI film; **c** surface morphology of CG-SCPE via in situ polymerization; **d** morphology for cross section of CG-SCPE



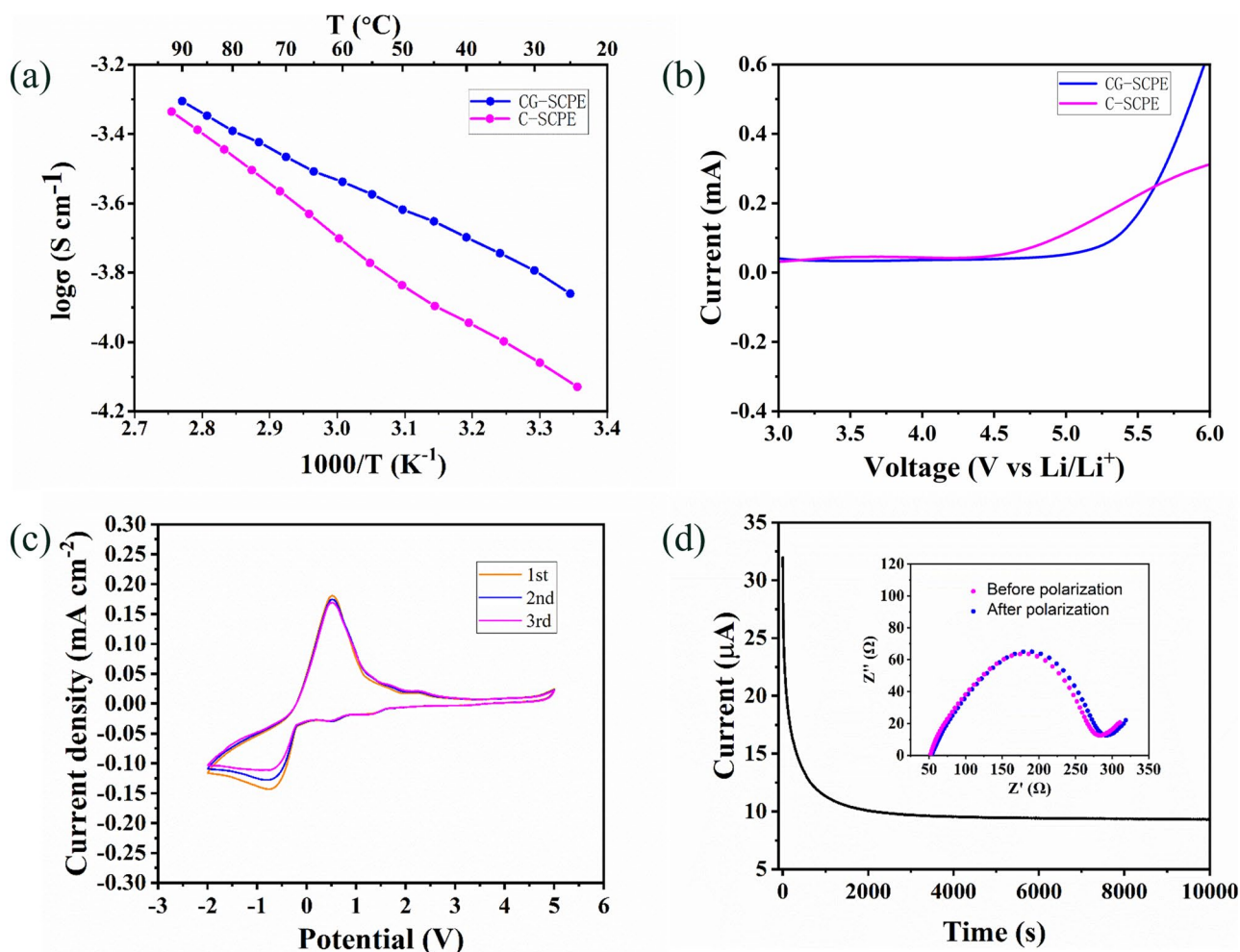


Fig. 3 Electrochemical properties of the CG-SCPE. **a** Ionic conductivities of CG-SCPE and C-SCPE; **b** LSV for electrolytes of CG-SCPE and C-SCPE at 25°C . **c** CV for electrolyte of CG-SCPE at 25°C

d Polarization curve along with the initial and steady-state electrochemical impedance diagram (inset) for the CG-SCPE at 25°C

can be used for high-voltage lithium metal batteries. The migration number of lithium ions ($t_{\text{Li}^{+}}$) for solid-state electrolyte is key to improve the battery rate capability. Here, a symmetrical Li/CG-SCPE/Li battery is assembled and $t_{\text{Li}^{+}}$ is measured from the DC polarization and electrochemical impedance spectroscopy (EIS) tests (shown in Fig. 3d). Specifically, from calculation based on Eq. (1), the $t_{\text{Li}^{+}}$ of the cross-linked polymer electrolyte CG-SCPE is measured to be 0.41, higher than that of common liquid electrolytes ($t_{\text{Li}^{+}} = 0.2\sim 0.3$), which is sufficient to support the rate performance improvement for battery.

The dynamic stability of the interface between lithium metal anode and cross-linked polymer electrolyte was studied utilizing polarization tests for Li/CG-SCPE/Li symmetric batteries. Specifically, galvanostatic cycling was performed on battery at current density of 0.1 mA cm^{-2} by charging and discharging for 1 h repeatedly to

verify CG-SCPE in stabilizing lithium metal deposition (Fig. 4). It exhibits stable performance for reversible lithium plating and stripping, with an overpotential of around 0.1 V. Even after 600 h, the overpotential remains stable (enlarged image), with no short circuit phenomenon witnessed during the entire galvanostatic cycling. Compared with the pristine lithium foil (Fig. 4b), the SEM image of the lithium metal anode after 600 h cycling (as shown in Fig. 4c) showed no significant changes with a smooth surface. This indicates that cross-linked polymer electrolytes could effectively inhibit the lithium dendrite growth.

To further explore why stable interface between the cross-linked polymer electrolyte and the lithium metal anode could be formed, the Li/CG-SCPE/Li battery was disassembled after cycling, and the surface chemistry of the lithium metal electrode was evaluated by X-ray photoelectron spectroscopy (XPS). The results are shown in the Fig. S4. XPS

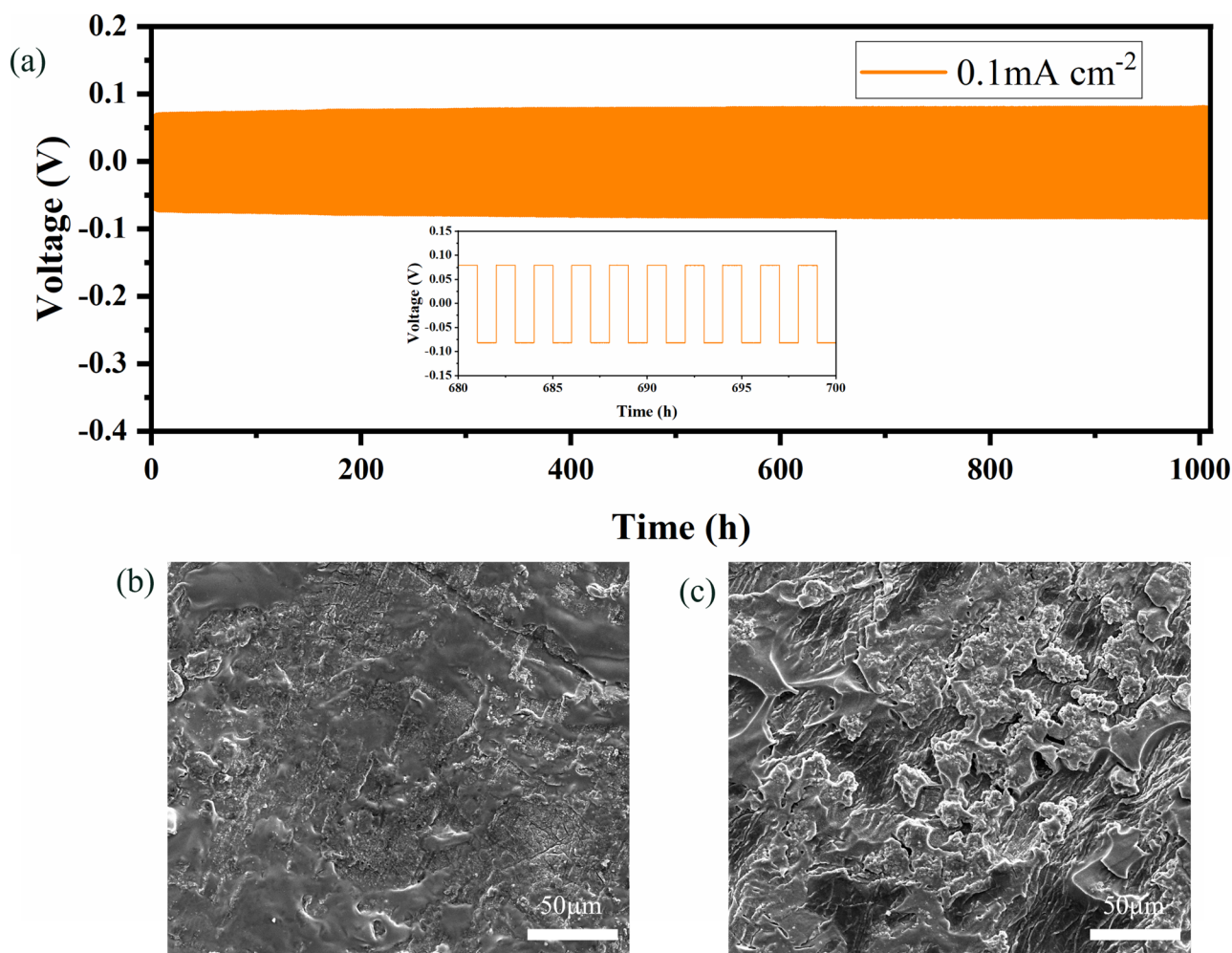


Fig. 4 Interface compatibility between CG-SCPE electrolyte with Li anode. **a** Galvanostatic cycling curves of the symmetric Li metal batteries with CG-SCPE at 0.1 mA cm^{-2} ; **b** SEM image for pristine Li

before cycling; **c** SEM image for Li anode after a cycling time of 200 h at 0.1 mA cm^{-2}

verifies the formation of LiF on lithium electrode surface, which could stabilize and improve interfacial compatibility. In addition, the SEI layer also includes organic substances of aliphatic carbon (C-C), ether carbon (C-OR), ROLi, and ROCO₂Li, as well as inorganic substances including Li₂O, LiOH, Li₂S₂, Li₂S, Li₂SO₃, and Li₂CO₃. We suppose that the LiF formation in SEI is introduced by liquid electrolyte of FEC added. To verify it, we compare the XPS data between CG-SCPEs with and without FEC added. It turns out that XPS of CG-SCPE without FEC presents a much weaker 1S signal for F element. It indicates that introduction of FEC promotes the LiF rich composition, which aids to form a stable and uniform SEI layer, beneficial for battery stability improvement and lithium dendrite growth inhibition. This cross-linked polymer electrolyte CG-SCPE in battery

presents long cyclability, indicating favorable compatibility between CG-SCPE and lithium metal anode.

We further tested the practical electrochemical performance of CG-SCPE in full cell of LiFePO₄/CG-SCPE/Li. The full cell of LFP/CG-SCPE/Li exhibits excellent cycling performance at 25 °C, as shown in the Fig. 5. At 0.1 C, the specific discharge capacity after 100 cycles remains 142 mA h g^{-1} , and the Coulombic efficiency is 99%. In the first five cycles, the specific capacity gradually stabilized, showing the initial activation of the electrolyte/Li metal interface. The rate performance of batteries using CG-SCPE as electrolyte was also studied at temperature of 25 °C, with results at different rates shown in Fig. 5c, d. At 0.1 C, 0.2 C, 0.3 C, 0.5 C, 1 C, and 2 C, the discharge specific capacities of the battery are 152 mA h g^{-1} , 149 mA h g^{-1} , 146 mA h g^{-1} , 142 mA h g^{-1} , 135 mA h g^{-1} , and 127 mA h g^{-1} , respectively.

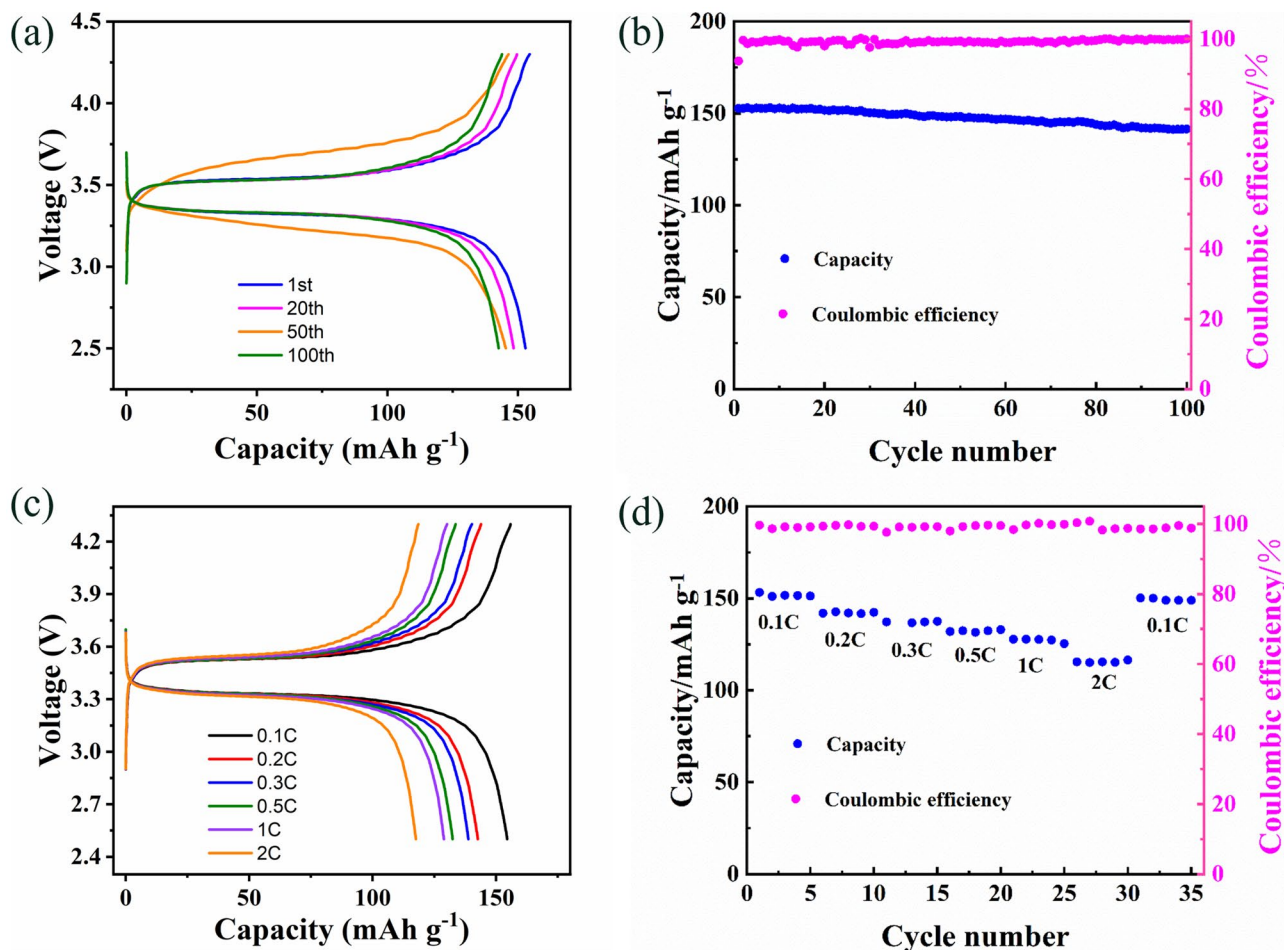


Fig. 5 Electrochemical properties of LiFePO₄/CG-SCPE/Li batteries. **a** Charge and discharge profiles of LiFePO₄/CG-SCPE/Li battery after different cycles at 0.1 C and 25 °C; **b** cycling stability of LiFePO₄/CG-SCPE/Li battery at 0.1 C and 25 °C; **c** charge and dis-

charge profiles of LiFePO₄/CG-SCPE/Li battery at various current rates and 25 °C. **d** Cycling stability of LiFePO₄/CG-SCPE/Li battery at various current rates at 25 °C

In tests, when the rate returns to 0.1 C after 2 C cycle, the discharge specific capacity can recover to its initial capacity value.

In addition, to evaluate the feasibility of CG-SCPE to pair high energy density cathode for lithium metal batteries, NCM532/CG-SCPE/Li batteries were also assembled and tested. Figure 6 shows the charging and discharging curves of a LiNi_{0.5}Co_{0.2}Mn_{0.3}O₂/CG-SCPE/Li full battery at 25 °C. The initial discharge capacity of this battery is 159.46 mA h g⁻¹. The Coulombic efficiency initially increased

steadily from 84.57% in the first few cycles and maintained over 99.5% throughout the following cycles. After 100 cycles, the discharge capacity of NCM532/CG-SCPE/Li decreased from the initial 159.06 to 127.6 mA h g⁻¹, with a capacity retention rate of 80.5%. Figure 6c, d shows the charge and discharge curves of NCM532/CG-SCPE/Li full cell at different current rates of 0.1 C, 0.2 C, 0.3 C, 0.5 C, 1 C, and 2 C, and at each rate, battery was tested for five cycles. The full battery manifests decent rate capability (Fig. 6d), while the polarization rises in response to the current density increase (Fig. 6c).

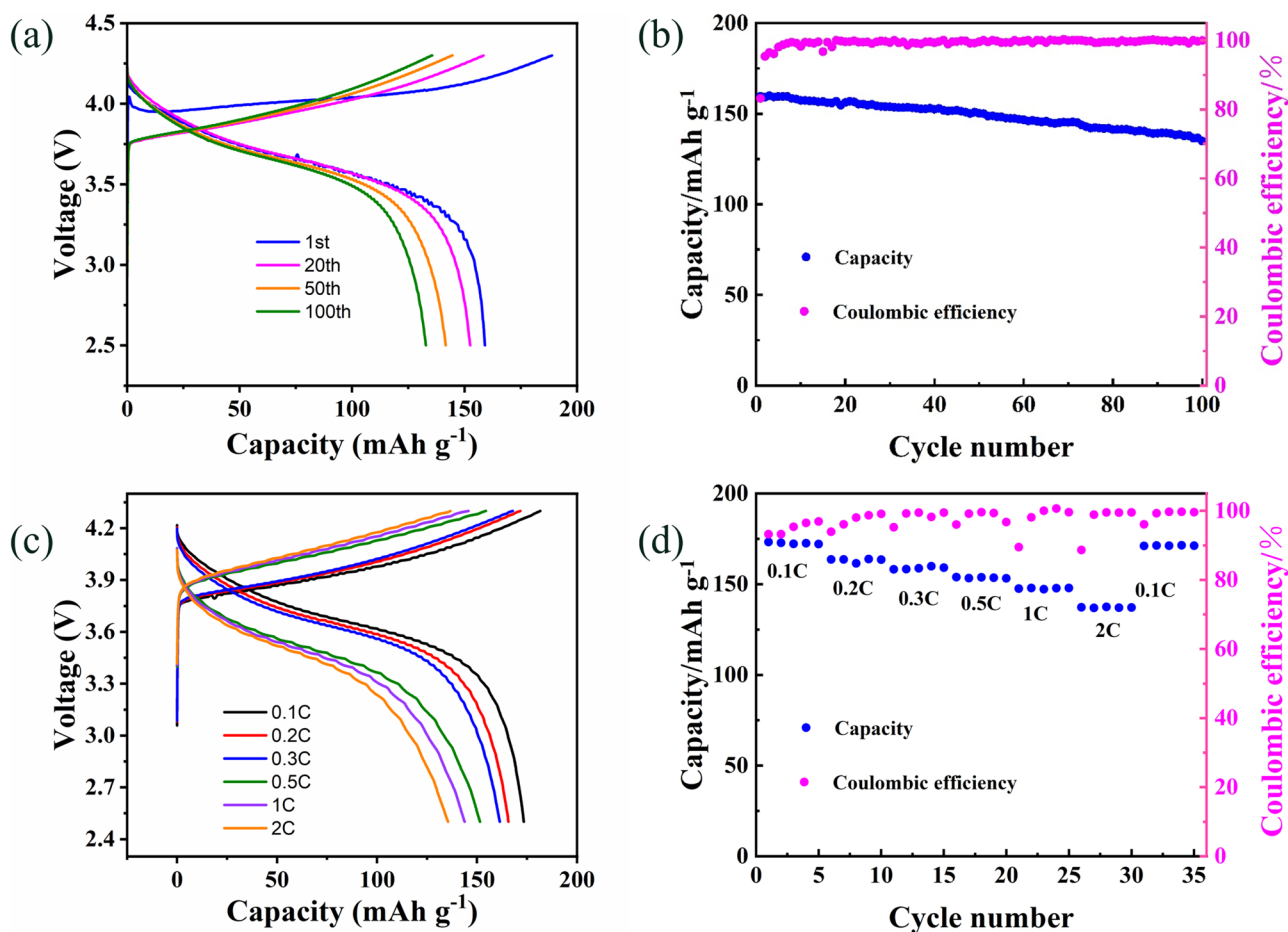


Fig. 6 Electrochemical properties of $\text{LiNi}_{0.5}\text{Co}_{0.2}\text{Mn}_{0.3}\text{O}_2/\text{CG-SCPE}/\text{Li}$ batteries. **a** Charge and discharge profiles of $\text{LiNi}_{0.5}\text{Co}_{0.2}\text{Mn}_{0.3}\text{O}_2/\text{CG-SCPE}/\text{Li}$ battery after different cycles at 0.2 C and 25 °C; **b** cycling stability of $\text{LiNi}_{0.5}\text{Co}_{0.2}\text{Mn}_{0.3}\text{O}_2/\text{CG-SCPE}/\text{Li}$ battery at 0.2

C and 25 °C; **c** charge and discharge profiles of $\text{LiNi}_{0.5}\text{Co}_{0.2}\text{Mn}_{0.3}\text{O}_2/\text{CG-SCPE}/\text{Li}$ battery at various current rates at 25 °C; **d** cycling stability of $\text{LiNi}_{0.5}\text{Co}_{0.2}\text{Mn}_{0.3}\text{O}_2/\text{CG-SCPE}/\text{Li}$ battery at various current rates at 25 °C

Conclusions

In this paper, a cross-linking gel polymer electrolyte was prepared by in situ polymerization initiated by thermal heating. This polymer electrolyte has excellent mechanical properties and outstanding interfacial compatibility with the cathode and lithium metal anode due to in situ polymerization. The ion conductivity of the polymer electrolyte CG-SCPE is $1.38 \times 10^{-4} \text{ S cm}^{-1}$, and it has an electrochemical stability window higher than 4.5 V vs. Li^+/Li . The $\text{LiFePO}_4/\text{Li}$ battery assembled with CG-SCPE exhibits excellent cycling performance, with an initial discharge capacity of 152 mA h g^{-1} and a Coulombic efficiency of 99% at a rate of 0.1 C. Meanwhile, $\text{LiNi}_{0.5}\text{Co}_{0.2}\text{Mn}_{0.3}\text{O}_2/\text{CG-SCPE}/\text{Li}$ batteries with high energy density cathode can also stably cycle at room temperature. Therefore, this polycarbonate-based interpenetrating polymer electrolyte is a potential candidate for the next generation of high-energy density lithium metal batteries.

Supplementary Information The online version contains supplementary material available at <https://doi.org/10.1007/s10008-024-05975-7>.

Funding Innovative Research Group Project of the National Natural Science Foundation of China, 22209027, Ziqiang Wang, Shenzhen Science and Technology Innovation Program, JCYJ20220530142806015, Ziqiang Wang, JCYJ20220818101008018, Ziqiang Wang, Shenzhen Peacock Plan, Tsinghua Shenzhen International Graduate School, JC2022002, Ziqiang Wang

Open Access This article is licensed under a Creative Commons Attribution 4.0 International License, which permits use, sharing, adaptation, distribution and reproduction in any medium or format, as long as you give appropriate credit to the original author(s) and the source, provide a link to the Creative Commons licence, and indicate if changes were made. The images or other third party material in this article are included in the article's Creative Commons licence, unless indicated otherwise in a credit line to the material. If material is not included in the article's Creative Commons licence and your intended use is not permitted by statutory regulation or exceeds the permitted use, you will need to obtain permission directly from the copyright holder. To view a copy of this licence, visit <http://creativecommons.org/licenses/by/4.0/>.

References

1. Etacheri V, Marom R, Elazari R, Salitra G, Aurbach D (2011) *Energy Environ Sci* 4:3243–3262
2. Motavalli J (2015) *Nature* 526:S96–S97
3. Yang C, Fu K, Zhang Y, Hitz E, Hu L (2017) *Adv Mater* 29:1701169
4. Zhao Q, Stalin S, Zhao CZ, Archer LA (2020) *Nat Rev Mater* 5:229–252
5. Xue Z, He D, Xie X (2015) *J Mater Chem A* 3:19218–19253
6. Liang J, Sun Y, Zhao Y, Sun Q, Luo J, Zhao F, Sun X (2020) *J Mater Chem A* 8:2769–2776
7. Liu T, Zhang J, Han W, Zhang J, Ding G, Dong S, Cui G (2020) *J Electrochem Soc* 167:070527
8. Li Z, Fu J, Zhou X, Gui S, Wei L, Yang H, Guo X (2023) *Adv Sci* 10:2201718
9. Jurkane A, Gaidukov S (2017) *Key Eng Mater* 721:18–22
10. Ding H, Lin B, Fang D, Dong Y, Wang S, Liu X, Meng G (2009) *J Alloy Compd* 474:364–369
11. Sun W, Zhang N, Mao Y, Sun K (2012) *J Power Sources* 218:352–356
12. Sun W, Zhang N, Mao Y, Sun K (2012) *Electrochem Commun* 20:117–120
13. Zhao Y, Fan L, Xiao B, Cai S, Chai J, Liu X, Liu Z (2023) *Energy Environ Mater* 6:e12636
14. Li Q, Sun X, Cao D, Wang Y, Luan P, Zhu H (2022) *Electrochem Energy Rev* 5:18
15. Ding P, Lin Z, Guo X, Wu L, Wang Y, Guo H, Yu H (2021) *Mater Today* 51:449–474
16. Zhang BH, Wu Y, Hou YL, Chen JZ, Ma Z, Zhao DL (2024) *Small* 20:2305322
17. Liu Q, Wang L, He X (2023) *Adv Energy Mater* 13:2300798
18. Guan HY, Lian F, Xi K, Ren Y, Sun JL, Kumar RV (2014) *J Power Sources* 245:95–100
19. Cui Y, Chai J, Du H, Duan Y, Xie G, Liu Z, Cui G (2017) *ACS Appl Mater Interfaces* 9:8737–8741
20. Cui Y, Liang X, Chai J, Cui Z, Wang Q, He W, Feng J (2017) *Adv Sci* 4:1700174
21. Geng Z, Huang Y, Sun G, Chen R, Cao W, Zheng J, Li H (2022) *Nano Energy* 91:106679
22. Mi YQ, Deng W, He C, Eksik O, Zheng YP, Yao DK, Wu ZP (2023) *Angew Chem Int Ed* 62:e202218621
23. Zheng J, Zhang J, Li W, Ge J, Chen W (2023) *Chem Eng J* 465:142796
24. Wang C, Li D, Liu N, Bai G, He W, Zhou X, Liu X (2023) *Polym Chem* 14:1094–1102
25. Vijayakumar V, Anothumakkool B, Kurungot S, Winter M, Nair JR (2021) *Energy Environ Sci* 14:2708–2788
26. Berthier C, Gorecki W, Minier M, Armand MB, Chabagno JM, Rigaud P (1983) *Solid State Ionics* 11:91–95
27. Tan J, Ao X, Dai A, Yuan Y, Zhuo H, Lu H, Lu J (2020) *Energy Storage Mater* 33:173–180
28. Nie K, Wang X, Qiu J, Wang Y, Yang Q, Xu J, Chen L (2020) *ACS Energy Lett* 5:826–832
29. Wan J, Xie J, Kong X, Liu Z, Liu K, Shi F, Cui Y (2019) *Nat Nanotechnol* 14:705–711
30. Duan J, Wu W, Nolan AM, Wang T, Wen J, Hu C, Huang Y (2019) *Adv Mater* 31:1807243
31. Isken P, Winter M, Passerini S, Lex-Balducci A (2013) *J Power Sources* 225:157–162
32. Nair JR, Destro M, Gerbaldi C, Bongiovanni R, Penazzi N (2013) *J Appl Electrochem* 43:137–145
33. Chen J, Wang C, Wang G, Zhou D, Fan LZ (2022) *Energy Mater* 2:200023
34. Ma Y, Ma J, Chai J, Liu Z, Ding G, Xu G, Chen L (2017) *ACS Appl Mater Interfaces* 9:41462–41472
35. Yu X, Wang L, Ma J et al (2020) Selectively wetted rigid–flexible coupling polymer electrolyte enabling superior stability and compatibility of high-voltage lithium metal batteries[J]. *Adv Energy Mater* 10(18):1903939
36. Zheng J, Li W, Liu X, Zhang J, Feng X, Chen W (2023) *Energy Environ Mater* 6(4):e12422
37. Zheng J, Li W, Zhang J, Sun Y, Chen W (2022) *ACS Sustain Chem Eng* 10(21):7158–7168

Publisher's Note Springer Nature remains neutral with regard to jurisdictional claims in published maps and institutional affiliations.